The Alcohol Dehydrogenase Kinetics Laboratory: Enhanced Data Analysis and Student-Designed Mini-Projects

Todd P. Silverstein*

Department of Chemistry, Willamette University, Salem, Oregon 97301, United States

S *Supporting Information*

ABSTRACT: A highly instructive, wide-ranging laboratory project in which students study the effects of various parameters on the enzymatic activity of alcohol dehydrogenase has been adapted for the upper-division biochemistry and physical biochemistry laboratory. Our two main goals were to provide enhanced data analysis, featuring nonlinear regression, and also to give students experience in experimental design. Students use appropriate kinetic and thermodynamic equations to fit their data from Michaelis–Menten plots, enzyme activity pH profiles, inhibitor and denaturant concentration profiles, and temperature-dependence plots. Experiments at the end of this project are designed and implemented by student pairs, thus preparing them for independent research.
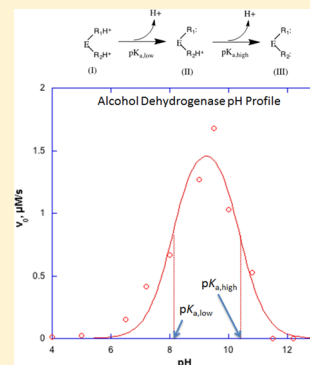
KEYWORDS: *Upper-Division Undergraduate, Biochemistry, Enzymes, Kinetics, UV-Vis Spectroscopy, Undergraduate Research*

■ INTRODUCTION

Alcohol dehydrogenase (ADH) is an ideal enzyme for the undergraduate biochemistry laboratory.[1−10] It is purified relatively easily from yeast[11−14] and liver,[15] is commercially available in purified form, and has been extensively studied and reviewed.[16−18] The enzyme has two substrates, alcohol and NAD^+, and is therefore more interesting to work with than the single-substrate or pseudo-first order enzymes that are typically studied in undergraduate laboratories.[9] An added advantage is that NADH, the reduced product, is a UV chromophore that is easily assayed spectrophotometrically. Because alcohol dehydrogenase is critical in both the catabolism of ingested ethanol and the production of ethanol by yeast, students have a natural interest in working with the enzyme.[2] This, in turn, allows faculty members to address the societal issue of psychoactive and addictive drugs,[1] along with important chemical and biochemical concepts.[1,2,13] Additionally, the inspiring story of Michaelis and Menten and their now well-known equation can be described to students.

In 2001, Bendinskas et al.[1] described a highly instructive, wide-ranging alcohol dehydrogenase experiment suitable for both the general chemistry and introductory biochemistry laboratory. In 2011, we received an NSF-TUES grant[19] to improve and expand our two-semester, integrated upper-division biochemistry laboratory.[20−27] One goal of this course is to give students experience in experimental design and prepare them for independent research. Another goal is enhanced data analysis, especially with nonlinear regression. Although almost all biochemistry laboratory courses include an enzyme kinetics project, very few do any data-fitting beyond the linearized Lineweaver–Burke plot. This leaves students in the dark with respect to the statistical weaknesses of linearizing nonlinear data, and the strengths of nonlinear regression. It also ignores the relatively simple thermodynamic and kinetic theory underlying the effects of pH, inhibitor, denaturant, and temperature on enzyme catalysis. The ADH kinetics project[1] has therefore been expanded with the two goals of enhanced data analysis and experimental design in mind.

■ PROCEDURE

Alcohol dehydrogenase catalyzes the reversible oxidation of alcohols to ketones or aldehydes (eq 1; a detailed mechanism of this reaction is summarized in Figure S1 in the Supporting Information):

$$\text{(1)}$$
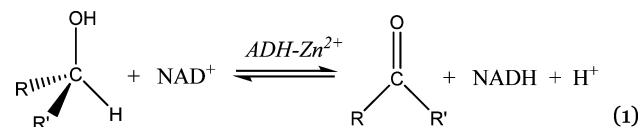
The reduced product NADH absorbs in the near UV region, with $\varepsilon_{340} = 6220$ M^{-1} cm^{-1}. In an attempt to avoid using UV spectrophotometry and expensive quartz cuvettes, Bendinskas et al.[1] coupled NADH to the redox mediators phenazine methosulfate (PMS) and 2,6-dichlorophenol-indophenol (DCIP), the latter of which bleaches from blue to colorless upon reduction. Although this coupling system should allow students to make measurements in the visible region, at 635 nm, it is difficult to use; often, our students saw no visible color

A

changes at all. Because visible lamps still have strong output at 340 nm, and UV-transparent disposable plastic cuvettes are widely available, the two redox mediators were eliminated and our students measured the production of NADH directly, at 340 nm. As long as students avoid contaminating their enzyme stock solutions with tap water, this simple experimental system gives robust, reproducible results.

Students performed 8−10 kinetic runs in a 3-h laboratory period, using Thermo-Electron Genesys-10 UV−vis spectrophotometers, one per student pair. For the purposes of curve-fitting, at least 6−7 data points are required, spread out along the x-axis. Therefore, kinetic runs were not repeated unless the results were clearly anomalous, and data points are thus plotted without error bars.

We use yeast ADH (*Saccharomyces cerevisiae*), purchased from Sigma (A-7011). Each student pair has a set of three adjustable micropipettors: 1000 μL, 100 or 200 μL, and 10 or 20 μL. This project has been run in the spring semester every year since 2007, with 6−18 students per semester, working in pairs; the approximate cost of the entire project is $2 to $3 per student. The project is allotted six, 3-h laboratory periods: (period 1) making buffer solutions and running Michaelis−Menten measurements at pH 9; (period 2) pH profile and Michaelis−Menten measurements at a suboptimal pH; (period 3) inhibitor concentration profile and Michaelis−Menten measurements on partially inhibited enzyme; (periods 4 and 5) student-designed further studies of two of the following ADH activity influences: temperature, ionic strength, denaturants, different alcohol substrates, concentrations of NAD$^+$ or enzyme; (period 6) data analysis. Further details and instructions for each day's activities can be found in the Supporting Information.

HAZARDS

Of the 15 enzyme inhibitor compounds and five denaturants that students may use in this laboratory project, most are skin and eye irritants; hence, gloves and safety goggles must be worn. Most of the compounds are also toxic by oral ingestion and/or inhalation. Barium^{2+}, cadmium^{2+}, copper^{2+}, and nickel^{2+} salts are oxidizers, and acetone and sodium dodecyl sulfate are highly flammable (category 3). Cadmium^{2+}, nickel^{2+}, acetamide, and thiourea are carcinogens; cadmium^{2+}, nickel^{2+}, imidazole, and thiourea damage fertility or the unborn child. Finally, cadmium^{2+}, copper^{2+}, nickel^{2+}, dinitrophenol, disulfiram, sodium dodecyl sulfate, thiourea, and Triton X-100 are toxic to aquatic organisms. All solutions of these compounds should be disposed into labeled waste containers.

DATA ANALYSIS

Michaelis−Menten Kinetics

Results published by Bendinskas et al. show that ADH activity saturates at about 0.1 M ethanol (Figure 1 presents typical data collected by a single student pair). The parameters (Table 1) that explain this hyperbolic saturation come from the Michaelis−Menten eq (eq 2),

$$v_0 = \frac{V_{max}}{1 + K_m/[S]_0} = \frac{k_{cat}[E]_0[S]_0}{K_m + [S]_0} \qquad (2)$$

where $K_m = S_{50}$ (substrate concentration that gives half-maximal velocity) $\approx K_d$(E·S), the equilibrium dissociation constant for the initial noncovalent enzyme−substrate complex; k_{cat} is the first-order rate constant for the subsequent rate-determining
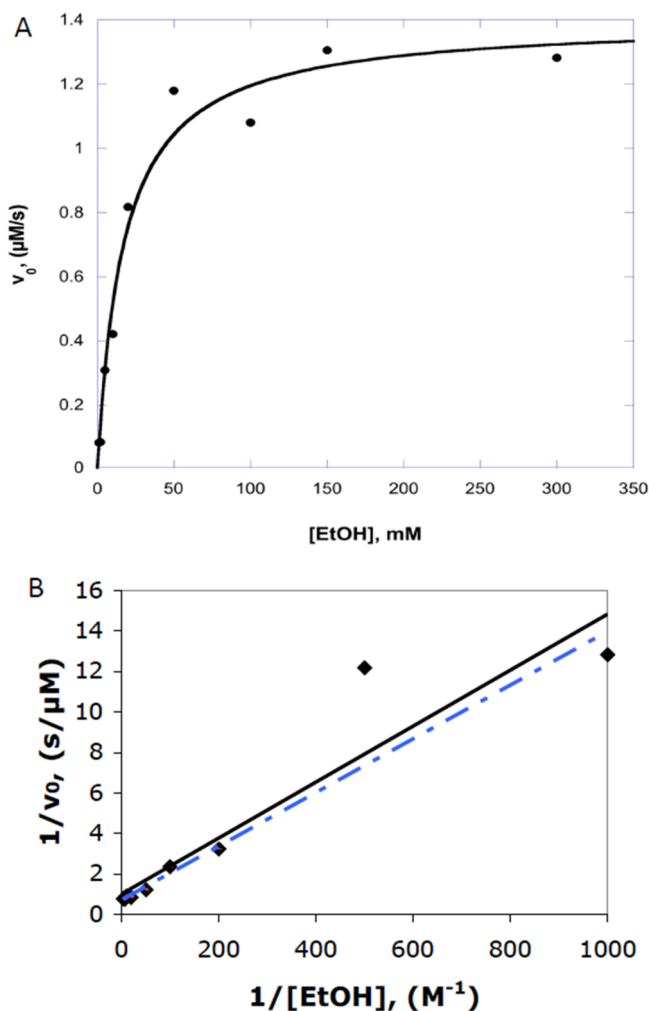
Figure 1. ADH kinetics plots for 17 nM ADH and 0.25 mM NAD$^+$ in 20 mM Tris, pH 9.0. Solid lines are fit to (A) eq 2, Michaelis−Menten plot; and to (B) eq 3, double-reciprocal plot. The dotted line in (B) omits the two lowest concentration (right-most) points from the linear regression; best-fit K_m and V_{max} values for this data set are listed in Table 1. Data are collected by a single student pair; each measurement was made only once; hence, error bars are absent.

conversion of bound substrate(s) to product(s); and $V_{max} = k_{cat}[E]_0 = v_0$ at infinite substrate concentration.

For a lower-division enzyme kinetics laboratory experiment, data analysis is often simplified by converting the nonlinear Michaelis−Menten eq (eq 2) to its linearized double-reciprocal form, eq 3. This allows students to calculate K_m and k_{cat} from linear regression results (Table 1).

$$1/v_0 = 1/V_{max} + (K_m/V_{max})\cdot(1/[S]_0) \qquad (3)$$

In this upper-division biochemistry project, students were instructed to compare the statistical reliability of the fitted parameters obtained from double-reciprocal linear regression vs hyperbolic saturation nonlinear regression. Our students use Kaleidagraph for nonlinear regression; other options (e.g., Excel-SOLVER, SigmaPlot, PeakFit) are discussed in the Instructor Notes in the Supporting Information. As an example, a single set of student results is analyzed thusly in Figure 1, panel B vs A. Because of the nonlinear nature of the reciprocal, experimental error in small values is magnified in the reciprocal;[28−33] this, in turn, means that unweighted double-

Table 1. Michaelis–Menten Parameters[a] for ADH at pH 9

Parameter	Michaelis–Menten (Figure 1A)	Double-reciprocal (Figure 1B, all points)	Double-reciprocal (omit low concentration points)
K_m, mM	17 ± 3	14 ± 10	18.6 ± 2.8
V_{max}, μM/s	1.40 ± 0.07	1.0 ± 0.7	1.40 ± 0.18
k_{cat}, s^{-1}	82 ± 4	60 ± 40	82 ± 11
R^2	0.974	0.88	0.969
y-intercept P-value	-	0.21	0.0006

[a]Best-fit parameters for data sets plotted in Figure 1. To compare these results from a single student pair with average results from 27 student pairs (2012–2015), see Table 2.

reciprocal plots often yield skewed fitted parameters.[3,28] It has been pointed out that the error-prone double-reciprocal plot is anachronistic;[29-33] however, it is still fairly common in the literature. Thus, it is important to have students perform both the linear and the nonlinear regressions; this allows them to explore for themselves the statistical unreliability of the double-reciprocal plot (Figure 1B), compared to the hyperbolically saturating Michaelis–Menten plot (Figure 1A).

For example, it is clear from the double-reciprocal plot that the two lowest concentration points (right-most in Figure 1B) deviate from the best-fit line much more than the other, higher-concentration points. Because the former two points lie at the high end of the x-axis, they exert undue weight on the fit. Furthermore, because both V_{max} and K_m are calculated from the y-intercept of the double-reciprocal plot (V_{max} = 1/intercept, K_m = slope/intercept), the reliability of this intercept is important. The y-intercept P-value for the double-reciprocal plot that includes all eight points (middle column of Table 1) is 0.21 (>0.05); hence, the statistical significance of the intercept is highly suspect. This can also be seen in the large uncertainties associated with K_m and V_{max} derived from this plot. After the two lowest-concentration points were removed, the statistical significance of the y-intercept improved dramatically (P = 0.0006, right-most column of Table 1), and the resulting Michaelis–Menten parameters more closely matched those from the nonlinear regression (left column of Table 1). Thus, students saw that nonlinear regression applied to the Michaelis–Menten plot gives more statistically reliable fitted kinetic parameters than linear regression applied to the double-reciprocal plot.

pH Dependence

To report the influence of pH on ADH activity, bar charts, which are appropriate for a project aimed at lower-division students, were previously used.[1] For upper-division students, pH profiles can be fitted assuming that the enzyme possesses two critical titratable acidic side chains that influence acitivity (Figure 2): For maximal activity, the first acidic group, R_1, must be deprotonated ($pK_{a,low}$) and the second group, R_2, must be protonated ($pK_{a,high}$). This is depicted as form (II) in Figure 2.

Only the monoprotonated form of the enzyme (II in Figure 2) is catalytically active; this form predominates at $pK_{a,low}$ < pH

< $pK_{a,high}$. Using the standard definition of the acid ionization constant, K_a, eq 4 is derived[34] (see Appendix 1 in the "Student Instructions" in the Supporting Information for a detailed derivation).

$$v_0 = \frac{v_0 \text{ (at optimal pH)}}{1 + 10^{(pK_{a,low}-pH)} + 10^{(pH-pK_{a,high})}} \quad (4)$$

In preparing for this part of the project, each student was responsible for making at least one of the 0.2 M buffer stock solutions. This was the first time that many of the students had to do this on their own, starting from scratch, giving them an excellent opportunity to (a) learn how to calibrate a pH meter; (b) think about the different ways to make a buffer solution and the reagents and glassware needed; (c) measure the effect of buffer dilution on pH; and (d) test the effect of buffer identity (by preparing two different buffers at the same pH, e.g., 0.20 M phosphate and Tris, both at pH 8.0).

Representative student results for an ADH pH profile (Figure 3) gave the following best-fit parameters: $pK_{a,low}$ = 8.10

Figure 3. pH profile for 17 nM ADH and 0.150 M ethanol in 20 mM buffer. Solid line is fit to eq 4; best-fit parameters are $pK_{a,low}$ = 8.10 ± 0.19; $pK_{a,high}$ = 10.37 ± 0.20; optimal pH = 9.23 ± 0.14; v_0 at pH optimum = 1.67 ± 0.19 μM/s; and R^2 = 0.94.

± 0.19; $pK_{a,high}$ = 10.37 ± 0.20; and optimal pH = 9.23 ± 0.14. Average results of 18 student pairs from 2012 to 2015 were as follows: $pK_{a,low}$ = 7.5 ± 0.7 (range, 6.6–8.6), $pK_{a,high}$ = 10.6 ± 0.4 (range, 9.8–11.3), and pH optimum = 9.1 ± 0.4 (range, 8.2–9.5).

Students interpreted the significance of the fitted $pK_{a,low}$ and $pK_{a,high}$ values in light of the following structural information.

Figure 2. Catalytically important acidic groups, R_1 and R_2.

The active site of ADH features a Zn^{2+} cation that is coordinated to cys_{46}−S:⁻, cys_{174}−S:⁻, his_{67}N:, and also to the oxygen atom of the ethanol substrate, in a tetrahedral arrangement.[16,17] Students often assigned one of the three zinc-bound acidic side chains as accounting for $pK_{a,low}$ = 7.5, because their nominal aqueous pK_a values are 8 (cys−SH) and 6−7 (hisNH⁺) and they must be deprotonated in order to bind Zn^{2+}. This provided an opportunity to entertain an important problem with these proposals. Although the nominal pK_a values for cysteine thiol and histidine imidazole are close to 7.5, the three active site groups are ionically bonded to the catalytic Zn^{2+}. Because of the resulting stabilization of their deprotonated forms, the cys−SH and hisNH⁺ side chains will have pK_a values that are 2−3 units *below* their aqueous values.[35] Thus, these three side chains cannot account for $pK_{a,low}$ = 7.5. However, crystal structures show[16,17] that the ethanol substrate molecule bound to ADH has its hydroxyl proton at the end of a hydrogen-bonding chain that begins with the basic side chain of histidine$_{51}$ (Figure 4), to which $pK_{a,low}$ = 7.5 could be reasonably assigned.
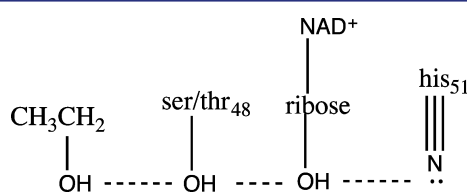
Figure 4. Proton transfer chain at the ADH active site. Ethanol (far left) and NAD⁺−ribose−OH are substrates; Ser/Thr$_{48}$ and His$_{51}$ are critical amino acid side chains. For a more detailed view of this proton transfer chain within the ADH active site, see Figure S1 in the Supporting Information.

To think about the identity of the side chain responsible for $pK_{a,high}$, students considered the remainder of the NAD⁺ substrate, which includes a pyrophosphate²⁻ moiety, along with a second ribose unit (see Appendix 1 in the "Student Instructions" in the Supporting Information). Lysine$_{228}$−NH$_3$⁺, which forms a hydrogen bond to a hydroxyl oxygen of the second ribose ring,[17] could account for $pK_{a,high}$ = 10.6.

At pH values other than the optimal, enzyme activity declines; this could be due to impaired substrate binding (higher K_m), impaired catalytic activity (lower k_{cat}), or both. Students investigated the effect of pH on Michaelis−Menten kinetic parameters by creating a Michaelis−Menten plot (0−0.3

M ethanol) at a suboptimal pH. Table 2 lists student results at pH 9 (optimal), and at pH's more acidic (pH 8) and more basic (pH 10) than optimal.

Loss of activity at the lower pH is due to impaired ethanol binding: K_m = 55 ± 15 mM at pH 8 vs 17 ± 3 mM at pH 9; V_{max} and k_{cat} are essentially the same at the two pH's. Thus, students may conclude that deprotonation of the amino acid side chain with $pK_{a,low}$ = 7.5 improves ethanol binding (lower K_m) but not the catalytic step (same V_{max} and k_{cat}). Although this conclusion seems less robust when considering averaged student results from 2012 to 2015 (Table 2 and Figure 5), in
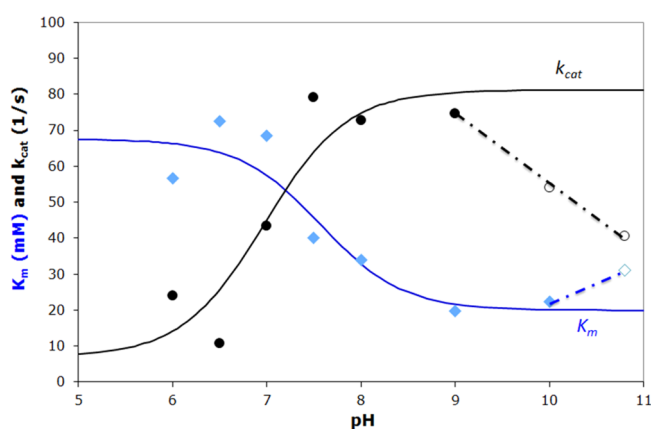
Figure 5. Influence of pH on ADH K_m (blue diamonds) and k_{cat} (black circles). Data are averaged student results from 2012 to 2015. Filled symbols are fit to eq 5. Open symbols at high pH (≥10) are not included in the curve-fit; dotted lines show the effects of alkaline-induced inhibition. For the sake of clarity, standard deviation error bars have been omitted here; they range from 5 to 30 mM for K_m points and from 2 to 35 s⁻¹ for k_{cat} points, and they can be seen in Figure S3 in the Supporting Information.

fact, 15 of 16 student pairs who studied pH < 9 found a significantly higher K_m at the lower pH. This can be seen as well in the range of K_m values at pH 8 (21−55 mM) vs pH 9 (7−35 mM).

The collected 2012−15 results presented in Figure 5 represent a pH titration of the parameters K_m and k_{cat}. The points can therefore be fit to the standard equation for pH titrations, eq 3. Best-fit parameters for the two data sets in Figure 5 are

Table 2. Effects of pH and Inhibitor (Cu^{2+}) on ADH Michaelis−Menten Kinetic Parameters[a]

	K_m, mM	V_{max}, μM/s	k_{cat}, s⁻¹	R^2	source
pH 8:	55 ± 15	1.49 ± 0.13	87 ± 8	0.963	2015, n = 1
average:	(34 ± 15)		(73 ± 27)		2012−2015, n = 8
range:	(21−55)		(30−100)		
pH 9:	17 ± 3	1.40 ± 0.07	82 ± 4	0.974	Figure 1A (2015, n = 1)
average:	(20 ± 9)		(75 ± 30)		2012−2015, n = 27
range:	(7−35)		(25−110)		
pH 10:	22 ± 9	1.16 ± 0.14	66 ± 8	0.893	2015, n = 1
average:	(22 ± 11)		(54 ± 14)		2012−2015, n = 3
range:	(10−33)		(20−60)		
pH 9, 20 μM Cu^{2+}	9 ± 5	0.84 ± 0.10	49 ± 6	0.75	Figure 6 (2015, n = 3)

[a]Results for 17 nM ADH, 0.25 mM NAD⁺, 0−0.3 M ethanol at pH 8−10. Values in parentheses represent the average and range of results from n student pairs, 2012−2015.

$$y_{pH} = y_{high\,pH} + \frac{y_{low\,pH} - y_{hipH}}{1 + 10^{(pH-pKa)}} \qquad (5)$$

for the K_m fit (blue line), K_m (high pH) = 20. ± 6. mM, K_m (low pH) = 68 ± 6 mM, pK_a = 7.6 ± 0.3 and R^2 = 0.905; for the k_{cat} fit (black line), k_{cat} (high pH) = 81 ± 12 s^{-1}, k_{cat} (low pH) = 7 ± 19 s^{-1}, pK_a = 7.0 ± 0.5 and R^2 = 0.86.

Combined student results from 2012 to 2015 (Figure 5) support a slightly different conclusion. As expected from Table 2, K_m does indeed rise from about 20 to 65 mM as pH falls (pK_a = 7.6: see blue diamonds in Figure 5) and k_{cat} is constant at about 75 s^{-1} from pH 7.5 to 9. However, below pH 7.5 k_{cat} declines dramatically to about 10 s^{-1} as pH falls (pK_a = 7.0: see black circles in Figure 5). This suggests that the side chain responsible for $pK_{a,low} \approx 7.5$, possibly histidine$_{51}$, serves two distinct functions: In its deprotonated form, it aids in both catalysis and in ethanol binding. The proton-transfer chain depicted in Figure 4 explains the former but not the latter.

Loss of activity at higher pH is due mainly to impaired catalysis: k_{cat} = 66 ± 8 s^{-1} at pH 10, vs 82 ± 4 s^{-1} at pH 9; K_m is essentially the same at both pH's. Hence, deprotonation of the side chain responsible for $pK_{a,high}$ impaired catalysis, but not ethanol binding. This supports the inference that the lysine$_{228}$ ammonium side chain, which helps to bind NAD$^+$ (but not ethanol), may be responsible for $pK_{a,high}$ = 10.6. Combined student results from 2012 to 2015 support this conclusion: Of the five student pairs who studied pH > 9, four found a significantly lower k_{cat} at the higher pH. In Figure 5, at pH 10.8 k_{cat} is about half its value at pH 7.5−9, whereas K_m at pH 10.8 is only slightly higher than its value at pH 9−10 (see unfilled symbols and dotted lines in Figure 5). Regarding the 63% loss of activity exhibited at pH 10.8 compared to pH 9, almost three-fourths of the loss is due to the decline in k_{cat}, as calculated from eq 2. Hence, high pH dramatically slowed catalysis while it only slightly hindered ethanol binding.

Enzyme Inhibition

Students chose one inhibitor to study, either a metal cation (Cd^{2+}, Al^{3+}, Ba^{2+}, Ni^{2+}, Cu^{2+}, Fe^{2+}), the chelator EDTA, or an organic compound (dithiothreitol, 4-nitrophenol, thiourea, acetamide, imidazole, N-ethyl maleimide, 4-methylpyrazole, or disulfiram).

Reversible enzyme inhibition can impact substrate binding (competitive inhibitors raise K_m), catalysis (mixed inhibitors lower k_{cat}), or both (uncompetitive inhibitors lower k_{cat} and K_m). From the fundamental kinetic equations describing these three types of reversible inhibition,[36] a general equation can be derived (eq 6, see Appendix 2 in the "Student Instructions" in the Supporting Information for derivations):

$$v_0 = \frac{V_{max}}{1 + \frac{K_m}{[S]_0} + x[I]_0} \qquad (6)$$

where V_{max} and K_m are those that apply to the control, uninhibited enzyme at the selected pH; $[S]_0$ and $[I]_0$ are the initial concentrations of substrate and inhibitor; and x represents the sensitivity of the enzyme to inhibitor (I)—a larger value of x signifies a steeper fall in v_0 as inhibitor is added. To make an inhibitor concentration profile, students selected particular substrate concentrations and a pH that would give good ADH activity (e.g., 0.25 mM NAD$^+$, 150 mM ethanol, pH 9), and measured activity at increasing concentrations of inhibitor. Defining IC$_{50}$ as the inhibitor concentration that gives

v_0(with inhibitor) = 1/2 v_0(control), eq 2 and eq 6 combine to give eq 7.

$$x = \frac{V_{max}\,(control)}{v_0\,(control)\cdot IC_{50}} = \frac{1 + (K_m\,(control)/[S]_0)}{IC_{50}} \qquad (7)$$

An effective inhibitor has a low IC$_{50}$ and a high enzyme sensitivity, x. Using eq 7 to substitute for x in eq 6 gives eq 8.

$$v_0 = \frac{v_0\,(control)}{\left(1 + \frac{[I]_0}{IC_{50}}\right)} \qquad (8)$$

Students fit their v_0 vs $[I]_0$ inhibitor profile data (Figure 6) to eq 8, and derived best-fit values for IC$_{50}$ and v_0(control). Using
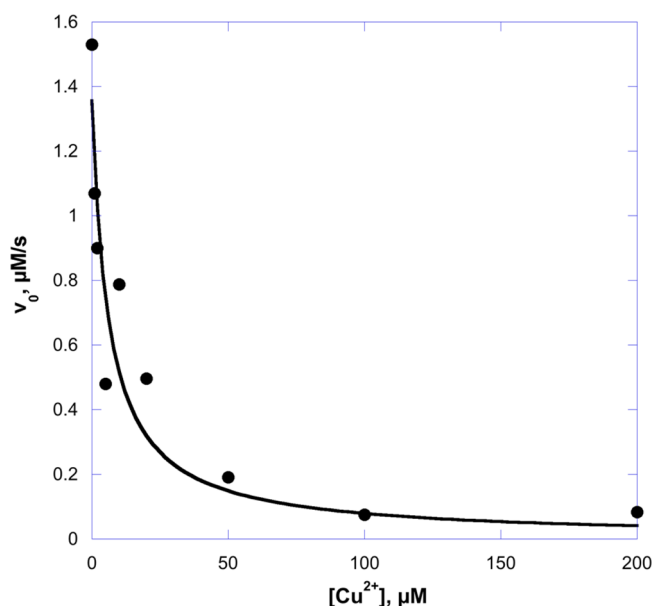
Figure 6. Inhibitor concentration profile for Cu^{2+}, with 17 nM ADH, 0.25 mM NAD$^+$, and 150 mM ethanol in 20 mM Tris, pH 9. Solid line is fitted to eq 8, with best fit parameters: IC$_{50}$ = 6.2 ± 2.5 μM; v_0 (control) = 1.36 ± 0.15 μM/s; R^2 = 0.879.

IC$_{50}$ along with their value of V_{max} (control) or K_m (control) determined from the pH 9 Michaelis−Menten plot (Figure 1A), students employed eq 7 to calculate the inhibitor sensitivity parameter x.

ADH is partially inhibited in the range 2−20 μM Cu^{2+} (Figure 6). A Michaelis−Menten plot in the presence of 20 μM Cu^{2+} at pH 9 (0−0.3 M ethanol, plot not shown) yielded best-fit parameters (Table 2, bottom row) that can be compared to the uninhibited enzyme. The inhibitor caused both K_m and V_{max} to decrease (by 2.0- and 1.7-fold, respectively) suggesting that Cu^{2+} functions as an uncompetitive inhibitor, binding only to the enzyme−substrate complex. The equilibrium constant for Cu^{2+} dissociation from the E·S complex, K_i', can be calculated in two ways: from the inhibitory constant ($\alpha_{ic}' \equiv 1 + [I]_0/K_i' =$ average of 2.0 and 1.7), and also from IC$_{50}$, eq 7, and the enzyme sensitivity parameter, x. (Relationships between x and enzyme−inhibitor dissociation constants are derived from the fundamental kinetic equations for the three types of reversible inhibition; see Figure S2 and Appendix 2 in the "Student Instructions" in the Supporting Information).

During the last two laboratory periods, students carried out further studies of ADH that they designed on their own. They

E

typically chose from two of the following parameters: denaturants, temperature, ionic strength, different alcohol substrates, and concentration of NAD⁺ or enzyme; other experiments were also considered.

Enzyme Denaturation

Students selected from the following denaturants: urea, guanidine hydrochloride, acetone, Triton X-100, or sodium dodecyl sulfate. The key parameters that describe the influence of denaturant on protein folding are IC_{50}, the concentration of denaturant that gives 50% unfolding, and $\Delta G^{\circ}_{U,H2O}$, the free energy of protein unfolding in the absence of denaturant.[37] The dependence of the equilibrium concentration of native/folded protein on denaturant concentration is given by eq 9 (see Appendix 3 in the "Student Instructions" in the Supporting Information for a derivation).[37] Proteins with a higher value of $\Delta G^{\circ}_{U,H2O}$ have a more stable native conformation that is more difficult to unfold; denaturants with a lower value of IC_{50} are more effective.

$$v_0 = \frac{v_{0,H_2O}}{1 + \exp\left[\frac{\Delta G^{\circ}_{U,H2O}}{RT}\left(\frac{[\text{denaturant}]}{IC_{50}} - 1\right)\right]} \tag{9}$$

Representative student results for an ADH urea concentration profile (Figure 7) had best-fit values $IC_{50} = 0.40$ M and
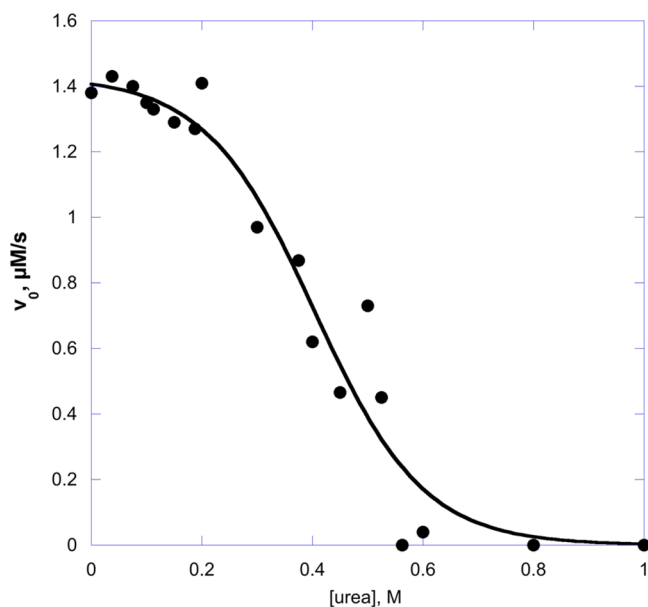
Figure 7. Influence of urea on ADH activity. Conditions are 17 nM ADH, 150 mM ethanol, 0.25 mM NAD⁺, 20 mM Tris, pH 9.0. Solid line is fit using eq 9; $IC_{50} = 0.404 \pm 0.024$ M; $\Delta G^{\circ}_{U,H2O} = 2.4 \pm 0.6$ kcal/mol; $v_{0,H2O} = 1.43 \pm 0.08$ μM/s; $R^2 = 0.951$.

$\Delta G^{\circ}_{U,H2O} = 2.4$ kcal/mol; the average of results from four student pairs over 2013–2015 was IC_{50} (urea) = 0.47 ± 0.21 M. Literature values for purified yeast ADH and several other well-studied enzymes fall within a fairly narrow range: $\Delta G^{\circ}_{U,H2O} = 3$–9 kcal/mol, and IC_{50} (urea) = 1.4–3.0 M.[37−41] Thus, student results were about 3-fold lower than previously reported. The commercial yeast ADH that our students use (Sigma A7011) is listed as ≥90% protein. It is possible that the non-ADH components destabilize ADH structure. Alternatively, it has been reported that apo-ADH (i.e., with Zn²⁺ removed from the active site) is significantly less

stable than holo-ADH (IC_{50} (urea) = 0.7 vs 1.4 M).[42] It is possible that the commercially obtained enzyme used in this study was partially demetallized.

Temperature Dependence: Arrhenius's Law versus Thermal Denaturation

Most enzymes have an optimal temperature, T_{opt}. As temperature increases up to T_{opt}, activity increases as described by Arrhenius's Law. However, above T_{opt} activity declines due to enzyme denaturation.[42] The effect of these two processes has been modeled (eq 10).[42]

$$v_0 = \frac{A_{app}e^{-E_{a(app)}/RT}}{1 + e^{(\Delta S^{\circ}_U/R)(1 - [T_U/T])}} \tag{10}$$

where $E_{a(app)}$, the apparent activation energy, is the sum of the activation energy for the rate-determining catalytic step and ΔH°_{bdg} for the fast enzyme–substrate binding equilibrium that precedes it;[42,43] ΔS°_U is the standard entropy of protein unfolding at 25 °C; T_U is the temperature at which the protein is 50% unfolded; and A_{app}, the apparent Arrhenius pre-exponential factor, equals the product of the pre-exponential factor for the rate-determining catalytic step times $e^{\Delta So(bdg)/R}$.[42,43] Equation 10 allows students to obtain best-fit values for T_{opt}, T_U, $E_{a(app)}$, ΔS°_U, and A_{app}.

The effect of temperature on ADH activity was previously depicted with a bar chart.[1] We include here a scatter plot version of those results (Figure 8). From the data in Figure 8,
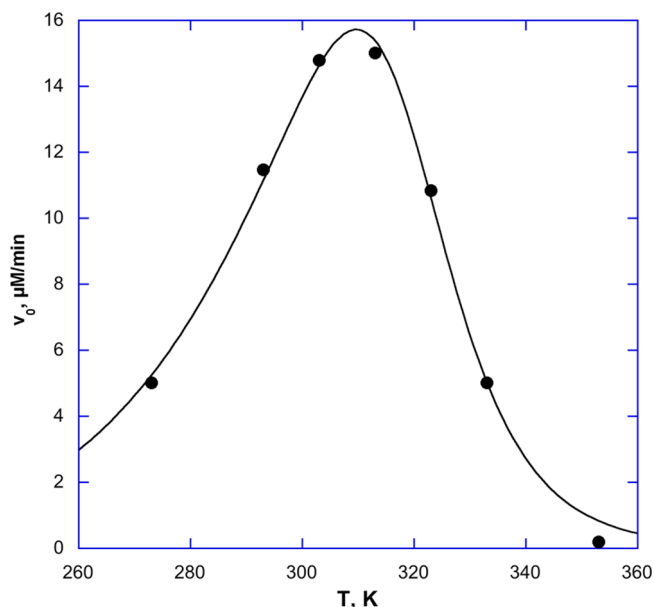
Figure 8. ADH activity as a function of temperature (0−80 °C), replotted from Bendinskas et al.[1] Figure 5. Solid line is a fit to eq 10; E_a (apparent) = 6.1 ± 0.7 kcal/mol; $\Delta S^{\circ}_U = 89 \pm 6$ cal/(mol·K); $T_U = 318.6 \pm 1.7$ K = 45.5 ± 1.7 °C; A (apparent) = (4 ± 5) × 10⁵ μM/s.

$T_{opt} = 311$ K = 38 °C, which matches literature values of 35−40 °C.[44−46] Interestingly, the best-fit $E_{a(app)}$ and ΔS°_U values obtained for ADH in Figure 8 are quite close to those obtained for lactate dehydrogenase (5.5 ± 2.4 kcal/mol and 90 ± 40 cal/(mol·K), respectively).[42] Although these two enzymes are not closely related evolutionarily (16% amino acid sequence identity and 22% sequence similarity), they are both NAD⁺-linked alcohol oxidases; hence, it would not be too surprising to

find enough structural similarities to explain this closeness in the unfolding parameters $E_{a(app)}$ and $\Delta S°_U$.

Other Enzyme Studies

Students who studied the influence of NAD^+ concentration used a Michaelis−Menten plot to determine K_m (NAD^+) and k_{cat}. The average of seven student pair results was $K_m = 0.44 \pm 0.13$ mM (range, 0.24−0.60 mM) and $k_{cat} = 240 \pm 50$ s^{-1} (range, 170−320 s^{-1}). Students who studied the influence of enzyme concentration found that activity is roughly linear with $[E]_0$, from 10 to 100 nM ADH. Students who studied the influence of ionic strength found that enzyme activity declines above about 0.5 M salt (e.g., NaCl, KCl, KNO$_3$). Bendinsaks et al.[1] reported ADH relative activities of alcoholic substrates thusly: ethanol > 1-propanol > butanol > methanol ≫ ethylene glycol. Note that methanol, 1-propanol, and ethylene glycol are everyday toxic compounds often encountered in medical practice. Methanol in particular exerts most of its toxicity via its ADH-oxidized product, formaldehyde; for this reason, a standard therapy for methanol poisoning is to administer ethanol. Students can analyze the kinetics of a competitive substrate as a variation on competitive inhibition. Our students found measurable ADH activity only for ethanol and 1-propanol. Students prepared Michaelis−Menten plots to determine K_m and k_{cat} for the oxidation of 1-propanol; the average of nine student pair results was $K_m = 26 \pm 5$ mM (range, 16−34 mM) and $k_{cat} = 45 \pm 20$ s^{-1} (range, 18−76 s^{-1}).

■ STUDENT EVALUATIONS

The two main goals of this expanded enzyme kinetics laboratory project were enhanced data analysis, and preparation for independent research; regarding laboratory skills, students gained experience in UV−vis spectrophotometry. Furthermore, because the final product of this laboratory project was a full formal report (including introduction, experimental methods, results, and discussion), students also worked on their written scientific communication skills. In the second semester laboratory course Experimental Biochemistry II, we have observed dramatic improvement in students' performance with data analysis and formal report writing. On the basis of these observations, as well as student feedback (see below), we feel that students have successfully achieved the learning outcomes outlined above.

Student feedback on this laboratory project was gathered using two instruments: (a) a single pre-mid-post laboratory skills assessment test (mainly multiple choice questions) was administered at the three time points. The test can be found in the Supporting Information. All but one of the 33 questions are multiple choice, and two of the questions call for solution preparation calculations, the rest being conceptual in nature. (b) A post-course evaluation questionnaire employed the 1 to 5 Likert scale, with '5' representing strongest agreement. Before the laboratory skills pre-test, students encountered enzyme kinetics in their biochemistry lecture course only; before the mid-test they completed the ADH kinetics laboratory project described here; and the post-test was administered after the second semester Experimental Biochemistry II course, which is devoted mainly to qPCR and the structure and dynamics of myoglobin and tRNA. The laboratory skills test included five questions relating to enzyme kinetics: three questions on hyperbolic saturation, and two on the K_m and V_{max} Michaelis−Menten parameters. For these questions, performance increased from 45% (pre) to 80% (mid) to 95% (post).

The Likert scale evaluation questionnaire also showed that the goals for this laboratory project were attained. Students expressed a strong sentiment (4.4 out of 5) that they were prepared for independent research even when they selected projects unrelated to biochemistry. They rated the course highly for helping them to develop skills in data analysis and interpretation (4.7), critical thinking and scientific reasoning (4.6), and writing scientifically (4.8). Two typical student comments expressed the sentiment that the course (and this project in particular): "enhance[d] my ability to use the instruments, computer programs, analyze data, and most importantly, to analyze the quality of published research". "This course confirmed that I enjoy working on experimental lab projects; [it] exposed me to the method of analysis for different types of biochemical inference, including forcing me to think about how to best analyze and interpret data."

■ ASSOCIATED CONTENT

ⓢ Supporting Information

The Supporting Information is available on the ACS Publications website at DOI: 10.1021/acs.jchemed.5b00610.

> Student Instructions: a detailed description of the experiment, including experimental protocols and appendices with derivations for fit equations (PDF, DOCX)
> Instructor Notes (PDF, DOCX)
> Laboratory skills assessment instrument (multiple choice) (PDF)
> Supplementary Figures S1, S2, and S3 (PDF, DOCX)

■ AUTHOR INFORMATION

Corresponding Author

*E-mail: tsilvers@willamette.edu.

Notes

The authors declare no competing financial interest.

■ ACKNOWLEDGMENTS

■ REFERENCES

(1) Bendinskas, K.; DiJiacomo, C.; Krill, A.; Vitz, E. Kinetics of alcohol dehydrogenase-catalyzed oxidation of ethanol followed by visible spectroscopy. *J. Chem. Educ.* **2005**, *82* (7), 1068−1070.

(2) Feinman, R. D. Ethanol Metabolism and the Transition from Organic chemistry to Biochemistry. *J. Chem. Educ.* **2001**, *78* (9), 1215−1220.

(3) Heydeman, M. T. Redox enzymes: a model coupled system. *Biochem. Soc. Trans.* **1991**, *19* (4), 401S.

(4) Carnahan, M.; Azbell, J.; Cox, K.; Espinosa, J.; Feaster, R.; Hirsch, R.; Lam, A.; Roller, S.; Steadman, B.; Toth, J.; Lee, M. Probing the Active Site of Yeast Alcohol Dehydrogenase through Microscale Yeast-Mediated Reductions of Acetophenone and Acetylpyridines. A

Collaborative and Research-Based Advanced Bioorganic Chemistry Laboratory Project. *J. Chem. Educ.* **2000**, *77* (3), 363−365.

(5) Nash, B. T. Determination of the subunit molecular mass and composition of alcohol dehydrogenase by SDS-PAGE. *J. Chem. Educ.* **2007**, *84* (9), 1508−1510.

(6) Prats, M.; Rodriguez, F. A Michaelis—Menten enzyme: Time correction introduced for computing kinetic parameters at low values of [S]/Km. *Biochem. Educ.* **1992**, *20* (3), 176−177.

(7) Taber, R. L.; Ladwig, J. W. The thermodynamic stability and catalytic activity of yeast alcohol dehydrogenase at different pH values: an undergraduate biochemistry investigation. *Biochem. Educ.* **1997**, *25* (3), 169−170.

(8) Taber, R. L. The competitive inhibition of yeast alcohol dehydrogenase by 2,2,2-trifluoroethanol. *Biochem. Educ.* **1998**, *26* (3), 239−242.

(9) Utecht, R. E. A kinetic study of yeast alcohol dehydrogenase. *J. Chem. Educ.* **1994**, *71* (5), 436−437.

(10) Walker, J. Spectrophotometric determination of enzyme activity: alcohol dehydrogenase (ADH). *Biochem. Educ.* **1992**, *20* (1), 42−43.

(11) Racker, E. Crystalline alcohol dehydrogenase from baker's yeast. *J. Biol. Chem.* **1950**, *184* (1), 313−319.

(12) Butler, P. J.; Jones, G. M. The preparation of alcohol dehydrogenase and glyceraldehyde 3-phosphate dehydrogenase from baker's yeast. *Biochem. J.* **1970**, *118* (3), 375−378.

(13) Suelter, C. H. Introduction to research: An undergraduate biochemistry laboratory. *Biochem. Educ.* **1982**, *10* (1), 18−21.

(14) Morgan, C.; Moir, N. Rapid microscale isolation and purification of yeast alcohol dehydrogenase using Cibacron blue affinity chromatography. *J. Chem. Educ.* **1996**, *73* (11), 1040−1041.

(15) Theorell, H.; Taniguchi, S.; Åkeson, Å; Skurský, L. Crystallization of a separate steroid-active liver alcohol dehydrogenase. *Biochem. Biophys. Res. Commun.* **1966**, *24* (5), 603−610.

(16) Hammes-Schiffer, S.; Benkovic, S. J. Relating protein motion to catalysis. *Annu. Rev. Biochem.* **2006**, *75* (1), 519−541.

(17) Trivic, S.; Leskovac, V. Structure and function of yeast alcohol dehydrogenase. *J. Serb. Chem. Soc.* **2000**, *65*, 207−227.

(18) Bullock, C. The biochemistry of alcohol metabolism - a brief review. *Biochem. Educ.* **1990**, *18* (2), 62−66.

(19) Silverstein, T. P.; Kirk, S. R. An Integrated, Instrument Intensive Project-Based Biochemistry Laboratory for Enhanced Student Learning and Research. **2011**, *DUE 1044737*.

(20) Silverstein, T. P.; Hudak, N. J.; Chapple, F. H.; Goodney, D. E.; Brink, C. P.; Whitehead, J. P. Scientific Communication and the Unified Laboratory Sequence. *J. Chem. Educ.* **1997**, *74* (2), 150−152.

(21) Silverstein, T. P.; Goodney, D. E. Enzyme-Linked Biosensors: Michaelis− Menten Kinetics Need Not Apply. *J. Chem. Educ.* **2010**, *87* (9), 905−907.

(22) Goodney, D. E.; Silverstein, T. P. Using the Tyrosinase-Based Biosensor To Determine the Concentration of Phenolics in Wine. *J. Chem. Educ.* **2013**, *90* (12), 1710−1712.

(23) Silverstein, T. P.; Kirk, S. R.; Meyer, S. C.; Holman, K. L. M. Myoglobin structure and function: A multiweek biochemistry laboratory project. *Biochem. Mol. Biol. Educ.* **2015**, *43* (3), 181−188.

(24) Kirk, S. R.; Silverstein, T. P.; Holman, K. L. M.; Taylor, B. L. Probing changes in the conformation of tRNA[Phe]: An integrated biochemistry laboratory course. *J. Chem. Educ.* **2008**, *85* (5), 666−673.

(25) Kirk, S. R.; Silverstein, T. P.; Holman, K. L. M. UV Thermal Melting Curves of tRNA[Phe] in the Presence of Ligands. *J. Chem. Educ.* **2008**, *85* (5), 674−675.

(26) Kirk, S. R.; Silverstein, T. P.; Holman, K. L. M. Metal-catalyzed cleavage of tRNA[Phe]. *J. Chem. Educ.* **2008**, *85* (5), 676−677.

(27) Kirk, S. R.; Silverstein, T. P.; Holman, K. L. M. Fluorescence Spectroscopy of tRNA[Phe] Y Base in the Presence of Mg^{2+} and Small Molecule Ligands. *J. Chem. Educ.* **2008**, *85* (5), 678−679.

(28) de Levie, R. When, why, and how to use weighted least squares. *J. Chem. Educ.* **1986**, *63* (1), 10−15.

(29) Martin, R. B. Disadvantages of double reciprocal plots. *J. Chem. Educ.* **1997**, *74* (10), 1238−1240.

(30) McNaught, I. J. Nonlinear Fitting to Kinetic Equations. *J. Chem. Educ.* **1999**, *76* (10), 1457−1457.

(31) Silverstein, T. P. Using a graphing calculator to determine a first-order rate constant. *J. Chem. Educ.* **2004**, *81* (4), 485.

(32) Silverstein, T. P. Quantitative Determination of DNA−Ligand Binding: Improved Data Analysis. *J. Chem. Educ.* **2008**, *85* (9), 1192−1193.

(33) Silverstein, T. P. Nonlinear and linear regression applied to concentration versus time kinetic data from Pinhas's sanitizer evaporation project. *J. Chem. Educ.* **2011**, *88* (11), 1589−1590.

(34) Hammes, G. *Enzyme Catalysis and Regulation*, student ed.; Academic Press: Orlando, FL, 1982; pp 54−58.

(35) Pace, C. N.; Grimsley, G. R.; Scholtz, J. M. Protein ionizable groups: pKa values and their contribution to protein stability and solubility. *J. Biol. Chem.* **2009**, *284* (20), 13285−13289.

(36) Nelson, D. L.; Lehninger, A. L.; Cox, M. M. *Lehninger Principles of Biochemistry*, 6th ed.; WH Freeman and Co.: New York, 2013; pp 207−210.

(37) Silverstein, T. P.; Blomberg, L. E. Probing Denaturation by Monitoring Residual Enzyme Activity and Intrinsic Fluorescence: An Undergraduate Biochemistry Experiment. *J. Chem. Educ.* **1992**, *69* (10), 852−855.

(38) Caffrey, M. S.; Daldal, F.; Holden, H. M.; Cusanovich, M. A. Importance of a conserved hydrogen-bonding network in cytochromes c to their redox potentials and stabilities. *Biochemistry* **1991**, *30* (17), 4119−4125.

(39) Knapp, J.; Pace, C. Guanidine hydrochloride and acid denaturation of horse, cow, and Candida krusei cytochromes c. *Biochemistry* **1974**, *13* (6), 1289−1294.

(40) Pace, C. N.; Laurents, D. V.; Thomson, J. A. pH dependence of the urea and guanidine hydrochloride denaturation of ribonuclease A and ribonuclease T1. *Biochemistry* **1990**, *29* (10), 2564−2572.

(41) Zhang, T.; Zhou, H. Comparison of inactivation and unfolding of yeast alcohol dehydrogenase during denaturation in urea solutions. *Int. J. Biol. Macromol.* **1996**, *19* (2), 113−119.

(42) Silverstein, T. P. Falling Enzyme Activity as Temperature Rises: Negative Activation Energy or Denaturation? *J. Chem. Educ.* **2012**, *89* (9), 1097−1099.

(43) Aledo, J. C.; Jiménez-Riveres, S.; Tena, M. The effect of temperature on the enzyme-catalyzed reaction: insights from thermodynamics. *J. Chem. Educ.* **2010**, *87* (3), 296−298.

(44) Zhao, Q.; Hou, Y.; Gong, G. H.; Yu, M. A.; Jiang, L.; Liao, F. Characterization of alcohol dehydrogenase from permeabilized brewer's yeast cells immobilized on the derived attapulgite nanofigers. *Appl. Biochem. Biotechnol.* **2010**, *160* (8), 2287−2299.

(45) Vanni, A.; Anfossi, L.; Pessione, E.; Giovannoli, C. Catalytic and spectroscopic characterisation of a copper-substituted alcohol dehydrogenase from yeast. *Int. J. Biol. Macromol.* **2002**, *30* (1), 41−45.

(46) Barzegar, A.; Moosavi-Movahedi, A. A.; Pedersen, J. Z.; Miroliaei, M. Comparative thermostability of mesophilic and thermophilic alcohol dehydrogenases: Stability-determining roles of proline residues and loop conformations. *Enzyme Microb. Technol.* **2009**, *45* (2), 73−79.